PHYSICAL REVIEW D **91,** 094025 (2015)

Tetraquark cusp effects from diquark pair production

Samuel H. Blitz[*] and Richard F. Lebed[†]

Department of Physics, Arizona State University, Tempe, Arizona 85287-1504, USA

(Received 26 March 2015; published 22 May 2015)

We present the first study of the cusp effect (the movement of resonant poles due to the proximity of multiparticle thresholds) caused by the creation of diquark-antidiquark pairs. The cusp profile for such states is obtained from constituent counting rules. We compare the effectiveness of diquark cusps in moving resonant poles with that from a phenomenological form commonly used for meson-pair creation and find that mesons tend to be more effective at lower energies (e.g., the $K\bar{K}$ threshold), while diquarks tend to be more effective at the charm [$X(3872)$] scales and above.

DOI: 10.1103/PhysRevD.91.094025 PACS numbers: 14.40.Rt, 12.39.Mk, 12.38.-t, 14.40.Pq

I. INTRODUCTION

One of the most important discoveries of the past year in hadron physics was the experimental confirmation by LHCb [1] of a new type of hadron joining the $\bar{q}q$ mesons and qqq baryons—the *tetraquark* ($\bar{q}q\bar{q}q$) resonance $Z_c^+(4430)$. In fact, this state is just one of an ever-growing menagerie of hadrons now believed to be tetraquarks, all of which have been observed since the 2003 discovery by Belle [2] of an unusually narrow charmoniumlike state, the $X(3872)$. However, until the discovery of charged states (now called Z_c), one could not be certain that the $X(3872)$ was not just an unusual conventional charmonium state or a hybrid $\bar{c}cg$; and until the observation of a phase δ increase by $\frac{\pi}{2}$ radians in the complex scattering amplitude in which Z_c is produced [1], one could not be certain that the states are true resonances as opposed to, say, kinematical reflections of t-channel exchanges. There now seems to be little doubt that the $Z_c^+(4430)$ is a tetraquark resonance with $J^P = 1^+$ quantum numbers and valence quark structure $\bar{c}c\bar{d}u$. In addition, all indications suggest that the charge-zero $X(3872)$ is a $J^P = 1^+$ $\bar{c}c\bar{q}q$ state, where $\bar{q}q$ is some linear combination of $\bar{u}u$ and $\bar{d}d$.

But waiting for the final confirmation of the tetraquark label did not preclude early speculation on the composition and structure of such states. The initial interpretation—and still the most prevalent one—is that the tetraquarks are dimeson molecules, bound together by color van der Waals-type forces (see Ref. [3] for a recent review). This interpretation is suggested by the proximity of the mass of several of the states to the corresponding two-meson thresholds. For example, $m_{X(3872)} - m_{D^{*0}} - m_{D^0} = -0.11 \pm 0.21$ MeV. However, several other tetraquark candidates lie just above such thresholds—clearly muddling the simple bound-state interpretation—and several others lie nowhere near any two-meson thresholds. Furthermore, the substantial prompt production cross section for the $X(3872)$ at colliders seems to be incompatible with the state being solely composed of loosely bound meson pairs [4,5]—even taking into account a substantial modification due to final-state interactions [6,7]. Another well-known interpretation is *hadrocharmonium* [8], in which an ordinary charmonium state lies at the core of a light-quark cloud, although the cohesiveness of such states, and the extent to which they mix with conventional charmonium states, is unclear.

In this work, we employ yet another noteworthy interpretation for the tetraquark states, that of a diquark-antidiquark (δ-$\bar{\delta}$) bound-state pair. Originally proposed for charmoniumlike tetraquarks in Ref. [9], the diquark picture has the advantage of possessing a much richer color dynamics (the diquarks necessarily being color nonsinglets), but it also has the potential drawback of producing many more tetraquark states than are currently observed. However, if one assumes that the dominant interactions are due to spin-spin couplings within each diquark, one can obtain a rather satisfactory accounting of the presently known tetraquark candidates [10].

One may wonder why the component quarks in a δ-$\bar{\delta}$ bound state do not immediately rearrange themselves into color-singlet $\bar{q}q$ pairs, returning one to the molecular picture. Indeed, the strength of the color force between quarks (or antiquarks) in SU(3)-color representations R_1 and R_2 coupling to a representation R is proportional to the combination of quadratic Casimirs given by $C_2(R) - C_2(R_1) - C_2(R_2)$. The only attractive channels are the $\bar{q}q$ singlet ($R_1 = \bar{\mathbf{3}}$, $R_2 = \mathbf{3}$, $R = \mathbf{1}$) and the qq antitriplet ($R_1 = R_2 = \mathbf{3}$, $R = \bar{\mathbf{3}}$), with the former being twice as strong as the latter.

Rather than treating the tetraquark as a metastable δ-$\bar{\delta}$ bound state, we proposed in Ref. [11] a new paradigm, in which the tetraquarks are the quantized modes of a color flux tube stretched between a rapidly separating δ (color-$\bar{\mathbf{3}}$) and $\bar{\delta}$ (color-$\mathbf{3}$) pair. This picture naturally explains why many, but not all, of the tetraquarks lie near hadron thresholds (energies at which the color string is allowed

[*]sblitz@asu.edu
[†]richard.lebed@asu.edu

to break); for example, the state $X(4632)$ lies only slightly higher than the lightest charmed-baryon $\Lambda_c^+\bar{\Lambda}_c^-$ threshold at 4573 MeV, and it decays dominantly to this baryon pair, as is explained by the fragmentation of the flux tube to a light $\bar{q}q$ pair. The widths of the states below this threshold are not especially large, because they hadronize by wave function overlaps with the mesons formed from quarks in $\bar{\delta}$ and antiquarks in the δ, which in turn can achieve a substantial separation (over 1 fm) if sufficient initial kinetic energy is imparted to the system, as in a B-meson decay. Evidence for this large separation is apparent in the decay of the $Z_c(4430)$, which greatly favors coupling to $\psi(2S)\pi$ rather than $J/\psi\pi$ [12]—even though the charmonium states have the same $J^{\rm PC} = 1^{--}$ quantum numbers and there is smaller phase space for the heavier (and spatially much larger) $\psi(2S)$.

This paper presents the first dynamical study of the δ-$\bar{\delta}$ tetraquark picture, using the well-known *constituent counting rules* [13–23], which determine the falloff scaling of hard exclusive processes in the high-energy regime. In essence, the counting rules predict that the cross sections, or equivalently, the form factors for processes at high values of Mandelstam s at fixed $\theta_{\rm cm}$, fall off as a power of s directly determined by the total number (incoming plus outgoing) of fundamental constituents participating in the hard subprocess. Here we are interested in comparing the effects of δ-$\bar{\delta}$ state production with that due to meson-meson states on the masses of tetraquark resonances coupled to them, using dispersion relation techniques. In another paper to appear [24], we will directly discuss the phenomenological uses of the cross-section scalings themselves.

The method to be used is the well-known *cusp effect*, in which the presence of thresholds for the opening of on-shell states coupled to resonances creates a modification to the self-energy function that tends to drag the bare resonant pole mass toward the threshold. The basic idea appears to have been known since the early 1960s but was first presented in its current form in the mid 1990s [25] and first applied to the new heavy exotics in 2008 [26]. Furthermore, recent calculations [27] show that these states cannot *just* be cusps (although ones in the $B\bar{B}$ system might be [28,29]); the presence of real resonances is required. In this paper we compare the effectiveness of this dragging effect due to the presence of both δ-$\bar{\delta}$ and two-meson thresholds and find first that the potential amount of shifting of resonant poles decreases for heavier-quark systems ($K\bar{K}$ vs $D\bar{D}^*$ vs $B\bar{B}^*$) and second that the δ-$\bar{\delta}$ states become more effective at pole dragging than two-meson states for the $D\bar{D}^*$ and $B\bar{B}^*$ thresholds associated with the new heavy exotic resonances. Since δ is not a color singlet, using a δ-$\bar{\delta}$ threshold in a QCD dispersion relation (where "on shell" usually means not only that the particles are not virtual but also asymptotically free) must be interpreted with some care; for the purposes of this calculation, we assert that the substantial δ-$\bar{\delta}$ separation advocated in Ref. [11] creates states that are in a sense "almost" free and therefore possess an on-shell threshold.

This paper is organized as follows. In Sec. II we briefly review the meaning and origin of the cusp effect and establish the mathematical formalism used for its implementation, with some details relegated to the Appendix. In Sec. III we address in greater detail the issue of whether diquark pairs truly produce physically meaningful thresholds. Section IV presents a brief overview of the constituent counting rules used to establish the large-energy scaling of the δ-$\bar{\delta}$ form factor. In Sec. V we describe the algebraic results for both the mesonic and diquark forms and present our numerical results in Sec. VI. In Sec. VII we summarize and indicate future directions.

II. CUSP EFFECT

The cusp effect has a rather straightforward origin in the analyticity of the self-energy functions $\Pi(s)$ that appear in the propagator of resonant or bound states and source the creation of their decay products. Closely following notation introduced in Refs. [25,26], we start with the propagator denominator

$$P^{-1}_{\alpha\beta}(s) = (M^2_{0,\alpha} - s)\delta_{\alpha\beta} - \Pi_{\alpha\beta}, \tag{1}$$

where the indices α, β label resonances that can mix; for simplicity, in this work we assume only unmixed propagating states and henceforth suppress this index. The sign of $\Pi(s)$ is chosen to match that appearing in the majority of quantum field theory texts (e.g., Ref. [30]); when positive, it is seen to correspond to an attractive interaction.

$\Pi(s)$ is analytic everywhere in the complex s plane except for cuts (or poles) along the positive real s axis that result from the opening of on-shell channels, which we label by i. Consider explicitly the creation of such two-particle states of masses $m_{1,i}$, $m_{2,i}$ via the form factors $F_i(s)$, conventionally normalized to unity at threshold, $s_{{\rm th},i} \equiv (m_{1,i} + m_{2,i})^2$. Defining the (dimensionful) coupling constant to state i as g_i, one has

$$\mathrm{Im}\Pi(s) = \sum_i g_i^2 \rho_i(s) F_i^2(s) \theta(s - s_{{\rm th},i}), \tag{2}$$

and ρ_i is the two-body phase-space factor given in terms of the c.m. momentum k_i or the Källén function λ by

$$\rho_i(s) \equiv \frac{2k_i}{\sqrt{s}} = \frac{\lambda^{\frac{1}{2}}(s, m^2_{1,i}, m^2_{2,i})}{s}. \tag{3}$$

Defining $s_{\rm th,1}$ as the lowest threshold (and therefore the cut extending to $s = \infty$ starting at the branch point $s_{\rm th,1}$ overlaps all others), one may apply Cauchy's theorem to a contour that goes around this cut, obtaining the standard unsubtracted dispersion relation,

$$\mathrm{Re}\Pi(s) = \frac{1}{\pi}\mathrm{P}\int_{s_{\mathrm{th},1}}^{\infty} ds' \frac{\mathrm{Im}\Pi(s')}{s'-s}, \tag{4}$$

where P indicates the standard Cauchy principal value prescription. For reasons to be discussed below, we find it useful to use the once-subtracted form (at $s=0$) of Eq. (4):

$$\mathrm{Re}\Pi(s) = \mathrm{Re}\Pi(0) + \frac{s}{\pi}\mathrm{P}\int_{s_{\mathrm{th},1}}^{\infty} \frac{ds'}{s'}\frac{\mathrm{Im}\Pi(s')}{s'-s}. \tag{5}$$

One notes immediately from Eqs. (2) and (3) that Im $\Pi(s)$ is zero on the real s axis for $s < s_{\mathrm{th},1}$ and positive for $s > s_{\mathrm{th},1}$. One further sees from Eq. (4) or (5) that the integrand in Re $\Pi(s)$ is positive for all $s < s_{\mathrm{th},1}$ since $s' - s > 0$ in the entire integration range and therefore acts as an attractive interaction. As shown below, explicit functional forms for $F(s)$ give rise to a positive Re $\Pi(s)$ that reaches a peak, or *cusp*, at $s_{\mathrm{th},1}$ and falls off in either direction, remaining always positive for $s < s_{\mathrm{th},1}$ but generally passing through the axis (and effectively creating a potential barrier) for some value of $s > s_{\mathrm{th},1}$. This effective attraction acts to pull the pole position of the propagator Eq. (1) toward $s_{\mathrm{th},1}$, a synchronization of the resonance with a threshold (although in Sec. VI we see some interesting exceptions to this expectation).

In the bulk of this work, for simplicity we specialize to the equal-mass case $m_{1,i} = m_{2,i} \equiv m_i$, which is rather closely satisfied for the cases of experimental interest. Full expressions analogous to the ones appearing in the text below are presented in the Appendix, where it is seen that the relevant expansion parameter is

$$\epsilon \equiv \left(\frac{m_{1,i} - m_{2,i}}{m_{1,i} + m_{2,i}}\right)^2. \tag{6}$$

For $X(3872)$, with $m_{1,i} = m_{D^0}$ and $m_{2,i} = m_{\bar{D}^{*0}}$, one finds $\epsilon = 1.35 \times 10^{-3}$. In the equal-mass case,

$$\rho_i(s) = \sqrt{1 - \frac{4m_i^2}{s}} = \sqrt{1 - \frac{s_{\mathrm{th}i}}{s}}, \tag{7}$$

and its analytic continuation for $s < s_{\mathrm{th},i} = 4m_i^2$ is

$$v_i(s) = \sqrt{\frac{4m_i^2}{s} - 1} = \sqrt{\frac{s_{\mathrm{th},i}}{s} - 1}. \tag{8}$$

To illustrate the cusp explicitly, let us consider the special case $F_i(s) = 1$ described in Ref. [26]. This particular choice is unphysical because unitarity and perturbative QCD require real hadronic form factors to fall off at large s, but it is an interesting toy model for cases in which the dispersion relation is dominated by the form factor near threshold. It is also interesting because the dispersion integrals can be carried out explicitly; the nonvanishing large-s behavior of $F_i(s)$ requires one to use the once-subtracted form Eq. (5) to obtain finite results at finite s. Allowing the constant $\mathrm{Re}\,\Pi_i(0) = -\frac{2}{\pi}$ to renormalize the pole mass M_0 in the propagator Eq. (1), one finds

$$\begin{aligned}\frac{\mathrm{Re}\Pi_i(s)}{g_i^2} &= \frac{\rho_i}{\pi}\ln\frac{1-\rho_i}{1+\rho_i} = -\frac{2\rho_i}{\pi}\tanh^{-1}\rho_i, \quad s \geq s_{\mathrm{th},i}, \\ &= -v_i + \frac{2v_i}{\pi}\tan^{-1}v_i, \quad s < s_{\mathrm{th},i}.\end{aligned} \tag{9}$$

Using Eqs. (7) and (8), note that the $\tan^{-1}$ and $\tanh^{-1}$ terms are analytic continuations of the same function of s in different regimes; the only unmatched term is $-v_i$, which is induced by analyticity of $\Pi(s)$ and the discontinuity of Im $\Pi_i(s_{\mathrm{th},i})$. In Fig. 1, we plot Eq. (9) [and Im $\Pi_i(s_{\mathrm{th},i})/g_i^2$] as a function of $s/s_{\mathrm{th},i}$ and see that the below-threshold term $-v_i$ is responsible for the cusp.

Cusp behavior also appears for more realistic choices of form factor $F_i(s)$, although the dispersion relation integrations must often be carried out numerically. Two features of the integrals hamper the convergence of numerical calculations: First, the integration range stretches to $s = \infty$, and, second, the denominator factor $s' - s$ produces a logarithmic singularity when $s > s_{\mathrm{th},i}$. A simple change of variable cures the first problem; noting from Eq. (7) that $s \in [s_{\mathrm{th},i}, \infty)$ maps to $\rho_i \in [0,1)$, one defines the integration variable ρ_i' analogously to Eq. (7), but with $s \to s'$. Then one finds the unsubtracted relation Eq. (4) to become

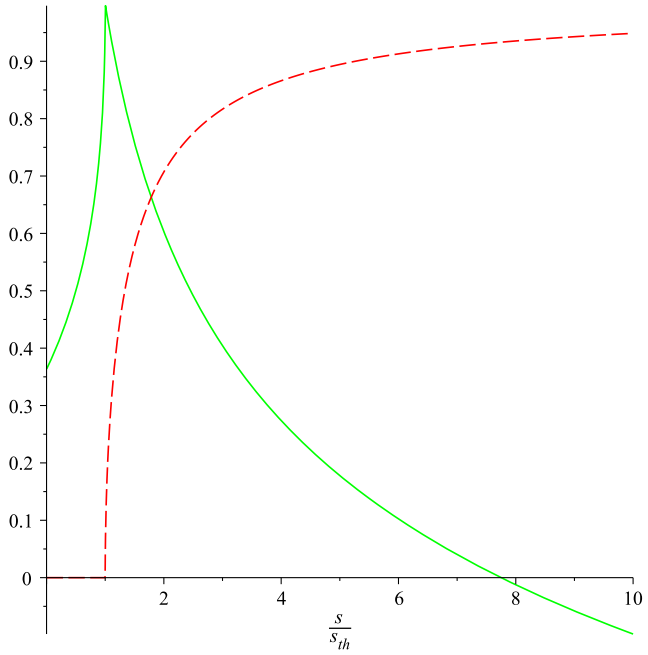

FIG. 1 (color online). The threshold cusp in Re $\Pi_i(s)/g_i^2$ (green, solid) and corresponding Im $\Pi_i(s)/g_i^2$ (red, dashed) for form factor $F_i(s) = 1$, as given by Eq. (9). s is expressed in units of $s/s_{\mathrm{th},i}$, and Re $\Pi_i(s)/g_i^2$ is shifted to equal 1 at $s = s_{\mathrm{th},i}$.

$$\frac{\mathrm{Re}\Pi_i(s)}{g_i^2} = \frac{2}{\pi}\frac{s_{\mathrm{th},i}}{s}\mathrm{P}\int_0^1 d\rho_i' \frac{\rho_i'^2}{1-\rho_i'^2}\frac{1}{\rho_i'^2-\rho_i^2}F_i^2(s'), \quad (10)$$

where [inverting Eq. (7)] $s' = s_{\mathrm{th},i}/(1-\rho_i'^2)$. In fact, the once-subtracted relation Eq. (5) becomes even simpler:

$$\frac{1}{g_i^2}[\mathrm{Re}\Pi_i(s) - \mathrm{Re}\Pi_i(0)] = \frac{2}{\pi}\mathrm{P}\int_0^1 d\rho_i' \frac{\rho_i'^2}{\rho_i'^2-\rho_i^2}F_i^2(s'). \quad (11)$$

Since, as discussed above, one expects Re $\Pi_i(s) \to 0$ as $s \to \infty$ for physical $F_i(s)$, no information is lost by using the once-subtracted and functionally simpler form Eq. (11). The logarithmic singularity does not arise for $s < s_{\mathrm{th},i}$; since $\rho_i^2 = -v_i^2$ according to Eqs. (7) and (8), one may rewrite the integrand factor in Eq. (11) for $s < s_{\mathrm{th},i}$ as the nonsingular form

$$\frac{\rho_i'^2}{\rho_i'^2-\rho_i^2} \to 1 - \frac{v_i^2}{\rho_i'^2+v_i^2}. \quad (12)$$

The logarithmic singularity for $s \geq s_{\mathrm{th},i}$ is readily handled via an integration by parts on the $1/(s'-s)$ factor in Eq. (5), followed by conversion to the integration variable ρ'. One obtains

$$\frac{1}{g_i^2}[\mathrm{Re}\Pi_i(s) - \mathrm{Re}\Pi_i(0)] = -\frac{1}{\pi}\int_0^1 d\rho_i'\left[F_i^2(s') + \frac{2s_{\mathrm{th},i}\rho_i'^2}{(1-\rho_i'^2)^2}\frac{dF_i^2(s')}{ds'}\right]\ln\frac{|\rho_i'^2-\rho_i^2|}{1-\rho_i^2}. \quad (13)$$

The singularity at $\rho_i = \rho_i'$ remains, but now it is integrable for any smooth $F_i^2(s)$ that asymptotes to zero as $s \to \infty$. Moreover, the nonlogarithmic part of this integral is just the exact differential $d[\rho_i(s')F_i^2(s')]$, the argument of which vanishes at $s' = s_{\mathrm{th},i}$ and also at $s' = \infty$ if $F_i^2(s')$ falls off faster than $1/\rho_i(s')$; in such a case, the (ρ_i'-independent) term $1-\rho_i^2$ in the logarithm may also be deleted. Since the function obtained from Eq. (5), i.e., the explicit left-hand side of (11) or (13), is central to our analysis, let us henceforth abbreviate it as $\pi_i(s) \equiv [\mathrm{Re}\Pi_i(s) - \mathrm{Re}\Pi_i(0)]/g_i^2$.

III. DO DIQUARK PAIRS HAVE THRESHOLDS?

Before proceeding, one must address the issue mentioned in the Introduction of whether a δ state, being colored, really possesses a well-defined mass and therefore whether the δ-$\bar{\delta}$ state really possesses a well-defined threshold. Strictly speaking, the quoted masses of colored particles like quarks depend upon the choice of renormalization scheme and therefore do not carry the same status of being observables as do meson masses. Nevertheless, quark masses are extracted using a variety of methods (quark models, lattice gauge theory, sum rules, etc.), and the numerical values thus obtained are bestowed with some degree of physical significance.

An elegant discussion of such issues appears in the classic text by Georgi [31] (Sec. 3.2); he considers a universe in which the strong coupling constant α_s is as small as α_{EM} but confinement still occurs. The scale Λ_{QCD} then becomes extremely large ($\simeq 10^{20}$ cm), and for all practical purposes, quarks would be just as visible in experiments as electrons and would possess easily determined quantum numbers such as mass. Georgi then continues the analysis by increasing Λ_{QCD} toward its physical $O(250\ \mathrm{MeV})$ value and argues that not until $\Lambda_{\mathrm{QCD}} \simeq \alpha_s m_q$ (including the running value of α_s) do quarks become inseparable from their hadrons, and hence hidden from view.

We take this lesson as our touchstone, that substantial physical separation implies identifiability as particles with well-characterized masses, even in the presence of confinement. The color dynamics allows diquarks to form as bound states, and kinematics permits them to separate a distance before being forced to hadronize. The salient question then becomes: How far is far enough, before the diquarks can reasonably be said to appear as identifiable particles possessing a well-defined mass threshold? We argue that this event occurs when the δ-$\bar{\delta}$ state can no longer be mistaken for one in which the diquark wave functions have substantial wave function overlap. Of course, the size of diquark wave functions is not at all a known quantity, but we can obtain a reasonable estimate by considering the size of mesons with analogous quark content. That is, instead of cu and $\bar{c}\bar{d}$ diquarks, we consider D mesons. Again, meson radii are not directly observable quantities, and the precise nature of the falloff of their wave functions with r is unknown, but at least in this case some calculations have been performed. For example, Ref. [32] calculates the electromagnetic charge radius of the D^+ to be 0.43 fm, rather smaller than charge radii of the unflavored mesons, due to the presence of the heavy c quark. One may expect the diquarks to be slightly larger because the initial color attraction between the quark components is smaller; however, the true size is dominated by some combination of nonperturbative gluodynamics and the heavy quark mass, so we expect the diquarks to be not much larger. We take from this result that 1 fm is not an unreasonable estimate for the onset of significant separation between the diquarks, and hence the identification of a well-defined diquark mass and pair-production threshold. Again, an important ingredient in this estimate appears to be the presence of heavy quarks, which might very well be related to the reason why exotics have first become clearly visible in the charm system.

Furthermore, as first pointed out in Ref. [25], the cusp effect treatment of the previous section holds at full strength

[as in Eq. (3)] only for thresholds of particles in a relative s wave. Only certain δ-$\bar{\delta}$ states will fall into this category, in precisely the same way that the conventional cusp effect is most prominent for thresholds of mesons produced in a relative s wave.

A very interesting question is how the diquark thresholds disappear if their separation is insufficient to prevent a large wave function overlap. We speculate that these thresholds gradually dissolve into correlations between the couplings to meson pairs to which the exotics preferentially decay, and such correlations would create a smeared "cusp" that would gradually disappear for smaller and smaller diquark separations. The exact separation at which such a structure first appears, and hence the assumption that a viable diquark cusp effect is supportable, is very much open to debate, but we believe 1 fm is a reasonable estimate. The diquark cusps studied in this paper are of course based upon an idealized picture of this behavior.

IV. CONSTITUENT COUNTING RULES

In this section we present a brief summary of the constituent counting rules developed over a number of years following the advent of perturbative QCD (pQCD) [13–23]. They reflect the underlying conformal features and scale invariance of the QCD coupling. More recently, they were derived nonperturbatively by Polchinski and Strassler [33] using AdS/QCD. A more thorough pedagogical introduction, particularly with an eye toward discerning exotic hadronic structure, is presented in Ref. [34]; here, we present an abridged discussion identifying the central points leading to the correct counting. In Ref. [35], the same authors show how to use the large-s scaling behavior to study the underlying generalized parton distributions and distribution amplitudes entering into these processes.

The constituent counting rules for large-angle scattering processes (i.e., those in which no kinematical variable is small due to the near collinearity of any particles) at high c.m. energy $\sqrt{s}$ originate from a remarkably simple source: Each of the individual constituents being scattered must be redirected through a finite angle by a large momentum transfer. In this limit, all constituent masses are negligible, and all three Mandelstam variables s, t, and $u \simeq -s - t$ are large, so that one may express all dimensionful quantities in powers of s and dimensionless coefficients as functions of t/s. In the pQCD picture, these deflections are accomplished through hard gluon exchanges; if leptons are included, then hard electroweak boson exchanges also appear. In the case of AdS/QCD, the counting rules reflect the twist dimension of the interpolating field at short distances.

For the moment, let us consider processes in which the constituents are all fermions. Then, assuming that each of the $n = n_{\text{in}} + n_{\text{out}}$ constituents shares a finite fraction of the total s, the leading-order Feynman diagrams require a minimum of $\frac{n}{2} - 1$ hard gauge boson exchanges and a minimum of $\frac{n}{2} - 2$ internal constituent propagators. These features supply factors of $1/s^{\frac{n}{2}-1}$ and $1/\sqrt{s}^{(\frac{n}{2}-1)}$ to the invariant amplitude $\mathcal{M}$, respectively. Noting that each external constituent fermion field carries a spinor normalization scaling as $s^{\frac{1}{4}}$, one sees that all of the fermion scaling factors cancel except for an overall factor s. In total,

$$\mathcal{M} \propto 1/s^{\frac{n}{2}-2}. \tag{14}$$

Assuming a conventional scattering process in which the constituents combine into two initial and two final particles, the cross section is given by

$$\frac{d\sigma}{dt} = \frac{1}{16\pi s^2}|\mathcal{M}|^2 \equiv \frac{1}{s^{n-2}} f\left(\frac{t}{s}\right), \tag{15}$$

where f has the appropriate mass dimension (M^{2n-8}) to match that (M^{-4}) of the left-hand side but does not itself scale as a power of s; its dimensionful factors are essentially the amplitudes describing the binding of the constituents into the composite states, i.e., decay constants.

Each external gauge boson introduced (e.g., turning an electroproduction process into photoproduction) removes two external fermion lines [$\sim(\sqrt{s})^2$] and one hard gauge boson propagator ($\sim 1/s$), leaving the form of the scaling formula for $\mathcal{M}$ and $d\sigma/dt$ invariant.

Hadronic form factors in the large-s regime can be studied analogously. For example, according to Eq. (14), the electromagnetic (or any other current-produced) form factor $F_X(s)$ appearing in the pair-production amplitude $\mathcal{M}$ for tetraquark states X scales as

$$F_X(s) \to \frac{1}{s^{\frac{1}{2}(1+1+4+4)-2}} = \frac{1}{s^3}. \tag{16}$$

While the origin of $1/s$ factors via hard exchanges is natural and simple, one may worry about technical complications in real perturbative QCD that disrupt the simple counting. These effects include the running of $\alpha_s(s)$, the renormalization-group scaling of the constituent distribution amplitudes [36,37], the presence of Sudakov logarithms [38–40], "pinch" singularities due to the vanishing of internal gluon propagators [41], and endpoint singularities occurring in configurations where some of the constituents do not share an $O(1)$ fraction of the hard scale s [42]. However, it is believed that the net result of these effects is not sufficiently severe as to change the leading s power scaling for exclusive processes.

V. MESONIC VS DIQUARK FORM FACTORS

The discussion of the previous section shows that the pair-production form factor $F_i(s)$ for a state with n constituents in the high-s regime scales as $1/s^{n-1}$. Of

course, this scaling is not expected to hold in the low-s region, particularly since confinement physics is not taken into account in this fundamentally perturbative approach.

A. Meson form factors

In the case of pair creation of conventional mesons, an exponential form is traditionally favored by phenomenological fits to data. For example, for $K\bar{K}$ production, Ref. [26] uses $F_i^2 = \exp(-k_i^2 R^2/3)$, where $R = 0.6$ fm, while for $B\bar{B}^*$ production, Ref. [29] uses $F_i^2 = \exp(-s/\beta_i^2)$ (once the coupling constant g_i is removed) and studies the choices $\beta_i = 0.4$, 0.5, and 0.7 GeV. To put these choices on a common footing, note from Eqs. (3) and (7) that $k_i = \frac{1}{2}\sqrt{s - s_{\mathrm{th},i}}$ and that the form in Ref. [29] can be normalized to unity at threshold by multiplying F_i^2 by a constant, $F_i^2 = \exp[-(s - s_{\mathrm{th},i})/\beta_i^2]$. Then the exponential form may be written as

$$F_i^2(s) = \exp\left(-\frac{\mu_i \rho_i^2}{1-\rho_i^2}\right), \tag{17}$$

where

$$\mu_i = \frac{s_{\mathrm{th},i} R^2}{12} = \frac{s_{\mathrm{th},i}}{\beta_i^2}, \tag{18}$$

so that $\mu_i = 0.738$ for Ref. [26] and $R = 0.6$ fm corresponds to $\beta_i = 1.14$ GeV. If k_i from Eq. (3) is identified with the nonrelativistic momentum $|\mathbf{k}_i|$, then one may compute the normalized nonrelativistic matter density $\rho(\mathbf{r})$ (not to be confused with ρ_i) as its Fourier transform,

$$\rho(\mathbf{r}) = \frac{1}{(2\pi\hbar)^3}\int d^3\mathbf{k}\, e^{-i\mathbf{k}\cdot\mathbf{r}/\hbar} F(\mathbf{k}^2), \tag{19}$$

giving in this case a Gaussian form:

$$\rho(\mathbf{r}) = \left(\frac{3}{4\pi R^2}\right)^{\frac{3}{2}} \exp\left(-\frac{3r^2}{4R^2}\right). \tag{20}$$

Inserting Eq. (17) into Eq. (11) leads to integrals for $\pi_i(s)$ that do not appear to be expressible in closed form except at special values of s. That the subtraction is performed at $s = 0$, and hence that $\pi_i(0) = 0$, is guaranteed by noting that $s = 0$ in Eq. (8) corresponds to $v_i^2 = -\rho_i^2 = \infty$. In terms of the Kummer (confluent hypergeometric) function $U(a, b, z)$, the function $\pi_i(s)$ and its slope $\pi_i'(s)$ can be computed at a few key values of s:

$$\begin{aligned}
&\pi_i(0) = 0, \qquad \pi_i'(0) = \frac{1}{2\sqrt{\pi} s_{\mathrm{th},i}} U\left(\frac{3}{2}, 0, \mu\right),\\
&\pi_i(s_{\mathrm{th},i}) = \frac{1}{\sqrt{\pi}} U\left(\frac{1}{2}, 0, \mu\right), \qquad \pi_i'(s_{\mathrm{th},i}^-) = \infty,\\
&\pi_i(\infty) = -\frac{1}{2\sqrt{\pi}} U\left(\frac{3}{2}, 1, \mu\right), \qquad \pi_i'(\infty) = 0.
\end{aligned} \tag{21}$$

These values can also be written as somewhat more complicated expressions in terms of the modified Bessel functions K_0 and K_1. Note especially the cusp $\pi'(s_{\mathrm{th},i}^-) = \infty$ (approaching from $s < s_{\mathrm{th},i}$), which follows directly from Eq. (11) for any $F_i^2(s)$ that is smooth at $s = s_{\mathrm{th},i}$ ($\rho_i = 0$). The slope $\pi'(s_{\mathrm{th},i}^+)$ (approaching from $s > s_{\mathrm{th},i}$), on the other hand, is generally finite (and negative) due to the smoothing effect of the principal-value prescription in Eq. (11).

It is important to note that a form factor $F_i^2(s)$ exponential in s cannot truly represent the full physical amplitude [43] in the entire complex s plane, since it produces an essential singularity for large s in some directions. Such behavior in dispersion relations would lead, for example, to a violation of causality. For our purposes, however, one may suppose that the behavior of $F_i^2(s)$ remains numerically close to the exponential form along a substantial portion of the real s axis but that the exact form contains a functional dependence in s (for example, the power-law falloff predicted by quark-counting rules) that restores the proper analytic behavior for all complex values of s.

B. Diquark form factors

The discussion of Sec. IV shows that the tetraquark form factor $F(s)$ at large s scales as $1/s^3$ due to the exchange of hard gluons needed to maintain the integrity of the exclusive tetraquark state. Indeed, the true scaling is $[\alpha_s(s)/s]^3$; however, the large-s scaling of α_s is logarithmic and therefore varies slowly compared to the power-law behavior, and henceforth is neglected.

The corresponding large-s behavior was not used for the mesonic case because one expects the four quarks produced at any low or intermediate s immediately to confine into two hadrons; the only color interactions between the two mesons are then the "color van der Waals" forces represented by final-state interactions. In the model of Ref. [11], however, the (colored) diquarks separate a significant distance before they are forced to hadronize, and so the fundamental color forces can be expected to remain active at much lower values of s than for the meson case. Since the natural scale at which the high-s scaling should become significant is given by the diquark mass $\sqrt{s_{\mathrm{th},i}} = 2m_\delta$, we model the diquark form factor by

$$F_i(s) = \left(\frac{s_{\mathrm{th},i}}{s}\right)^3, \tag{22}$$

which of course is properly normalized, $F_i(s_{\mathrm{th},i}) = 1$. Using Eqs. (3) and (19), the matter density associated with this form factor is

$$\rho(\mathbf{r}) = \frac{1}{32\pi r_C^3}\left(1 + \frac{r}{r_C}\right)e^{-r/r_C}, \tag{23}$$

where r_C is the diquark Compton wavelength $1/m_\delta$.

In this case, the integrals in $\pi_i(s)$ can be performed in closed form. First, for $s > s_{\mathrm{th},i}$, one finds

$$\pi_i(s) = \frac{1}{\pi}\left\{-\rho_i(1-\rho_i^2)^6 \ln\left(\frac{1+\rho_i}{1-\rho_i}\right) + \frac{2048}{3003} - 2\rho_i^2\left(\frac{793}{231} - \frac{667}{63}\rho_i^2 + \frac{562}{35}\rho_i^4 - \frac{66}{5}\rho_i^6 + \frac{17}{3}\rho_i^8 - \rho_i^{10}\right)\right\}. \tag{24}$$

In the $s < s_{\mathrm{th},i}$ case, we define [using Eq. (8)] the parameter

$$\gamma_i \equiv \frac{s}{s_{\mathrm{th},i}} = \frac{1}{1+v_i^2}, \tag{25}$$

which varies from $0 \to 1$ as s increases from $0 \to s_{\mathrm{th},i}$. One then computes

$$\pi_i(s) = \frac{1}{\pi\gamma_i^6}\left\{-\sqrt{\frac{1-\gamma_i}{\gamma_i}}\left[\frac{\pi}{2} - \tan^{-1}\left(\frac{\frac{1}{2}-\gamma_i}{\sqrt{\gamma_i(1-\gamma_i)}}\right)\right] + 2\left(1 - \frac{1}{3}\gamma_i - \frac{2}{15}\gamma_i^2 - \frac{8}{105}\gamma_i^3 - \frac{16}{315}\gamma_i^4 - \frac{128}{3465}\gamma_i^5 - \frac{256}{9009}\gamma_i^6\right)\right\}. \tag{26}$$

These precise forms are not terribly illuminating in their own right, but they can be used to compute various limits for purposes of comparison with the mesonic case. For example, Eq. (26) appears to have a very strong singularity at $\gamma_i = 0$ ($s = 0$), but the complicated polynomial in γ_i has precisely the right form to cancel all the terms in the expansion of the $\tan^{-1}$ expression in powers of γ_i to the same order to give $\pi_i(0) = 0$, and furthermore to give a finite value at $\gamma_i = 1$ ($s = s_{\mathrm{th},i}$) that matches the one from Eq. (24) at $\rho_i = 0$, but with a derivative from below that is infinite. In comparison with Eq. (21),

$$\pi_i(0) = 0, \qquad \pi_i'(0) = \frac{2048}{45045\pi s_{\mathrm{th},i}},$$
$$\pi_i(s_{\mathrm{th},i}) = \frac{2048}{3003\pi}, \qquad \pi_i'(s_{\mathrm{th},i}^-) = \infty,$$
$$\pi_i(\infty) = -\frac{512}{9009\pi}, \qquad \pi_i'(\infty) = 0. \tag{27}$$

VI. NUMERICAL RESULTS

In this section we present explicit numerical comparisons of the effects of threshold cusps due to mesons compared to those due to δ-$\bar{\delta}$ pairs. But first, we make a few comments about how best to present and interpret these effects.

While it is rather suggestive to describe the attractive cusp in $\mathrm{Re}\,\Pi_i(s)$ at $s = s_{\mathrm{th},i}$ as a potential well that attracts a bare pole to the threshold, it is important not to be overly seduced by the analogy with a configuration-space potential well, which always attracts a particle to the vicinity of its minimum. The intuition one develops for the cusp effect needs to be more nuanced. In fact, the entire portion of the cusp over which $\mathrm{Re}\,\Pi_i(s)$ is positive and appreciable in magnitude provides a source of attraction for the pole. For example, even if the bare pole mass sits exactly at $M_0 = \sqrt{s_{\mathrm{th},i}}$, the cusp can drive the pole mass to a value slightly larger than $\sqrt{s_{\mathrm{th},i}}$; such an effect is visible in the results in Table II of Ref. [26].

The corrected pole mass M_{pole} is the pole of the propagator, i.e., the zero of Eq. (1). As the physical resonance pole first appears on the second Riemann sheet, one must take care to choose the sign corresponding to the correct branch in the self-energy function $\Pi_i(s)$. The effect of the threshold cusp on the position of a pole can then be described succinctly in terms of the dimensionless ratios $M_0/\sqrt{s_{\mathrm{th},i}}$ and $M_{\mathrm{pole}}/\sqrt{s_{\mathrm{th},i}}$. In light of the observation that the whole profile of the cusp is active in dragging M_0 to M_{pole}, one expects that the cusp is most effective in dragging the pole if either the coupling g_i to the opening threshold is large or the cusp function $\mathrm{Re}\,\Pi_i(s)$ is broad in s. The question of whether the mesonic or diquark threshold cusp is more effective in pole dragging thus comes down to these two criteria.

To exhibit the effectiveness of the cusp numerically, we first superimpose two plots in Fig. 2. The first is a sample (diquark) cusp $\pi_i(s)$ with $g_i = 0.370$ GeV and $\sqrt{s_{\mathrm{th},i}} = 3.872$ GeV, which uses the abscissa $x \equiv s/s_{\mathrm{th},i}$. Its peak is normalized at threshold ($x = 1$) to match that of the second plot, which uses the abscissa $x \equiv M_0/\sqrt{s_{\mathrm{th},i}}$ and an ordinate that gives a measure of the effectiveness of the cusp in dragging the pole, chosen to be

$$y \equiv \frac{M_{\mathrm{pole}} - M_0}{\sqrt{s_{\mathrm{th},i}}}. \tag{28}$$

The pole-dragging function y very closely follows the shape of the cusp but does not precisely match it.

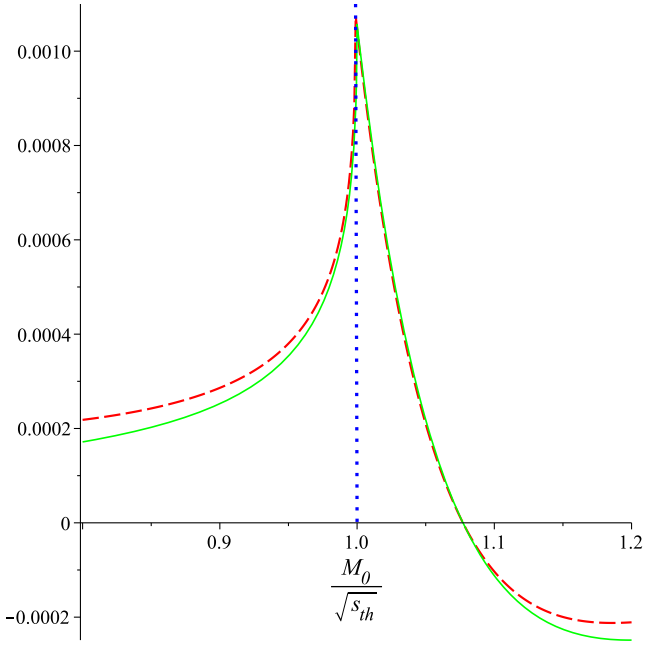

FIG. 2 (color online). A sample threshold cusp (solid, green) using the diquark form presented in Sec. V B, plotted as a function of $x \equiv \sqrt{s/s_{\mathrm{th},i}}$. Its peak normalization is chosen to match that of the overlaid (dashed, red) pole-dragging effect of this cusp, $y \equiv (M_{\mathrm{pole}} - M_0)/\sqrt{s_{\mathrm{th},i}}$, with $g_i = 0.370$ GeV and $\sqrt{s_{\mathrm{th},i}} = 3.872$ GeV, and plotted as a function of a second abscissa $x \equiv M_0/\sqrt{s_{\mathrm{th},i}}$. Also plotted is the line $y = 1 - x \equiv 1 - M_0/\sqrt{s_{\mathrm{th},i}}$ (dotted, blue) dividing Regions 1 and 2, as defined in the text.

Qualitatively, this result means that the cusp does indeed attract the pole over a significant range of $M_0/\sqrt{s_{\mathrm{th},i}}$. To consider the effect more carefully, we characterize regions of the plot:

(1) $\frac{M_0}{\sqrt{s_{\mathrm{th},i}}} < \frac{M_{\mathrm{pole}}}{\sqrt{s_{\mathrm{th},i}}} < 1$: attraction of below-threshold pole toward $s_{\mathrm{th},i}$;
(2) $\frac{M_0}{\sqrt{s_{\mathrm{th},i}}} < 1 < \frac{M_{\mathrm{pole}}}{\sqrt{s_{\mathrm{th},i}}}$: attraction of below-threshold pole past $s_{\mathrm{th},i}$;
(3) $1 < \frac{M_0}{\sqrt{s_{\mathrm{th},i}}} < \frac{M_{\mathrm{pole}}}{\sqrt{s_{\mathrm{th},i}}}$: repulsion of above-threshold pole from $s_{\mathrm{th},i}$;
(4) $1 < \frac{M_{\mathrm{pole}}}{\sqrt{s_{\mathrm{th},i}}} < \frac{M_0}{\sqrt{s_{\mathrm{th},i}}}$: attraction of above-threshold pole toward $s_{\mathrm{th},i}$.

The other two possibilities, i.e., repulsion of a below-threshold pole from $s_{\mathrm{th},i}$ and attraction of an above-threshold pole past $s_{\mathrm{th},i}$, do not occur for cusp functions of the types considered here. The interesting possibility (Region 2) mentioned above, of the cusp causing a below-threshold pole to overshoot threshold, is represented in Fig. 2 as the sliver of the plot between the line $1 - x$ and the vertical line $x = M_0/\sqrt{s_{\mathrm{th},i}} = 1$. At these input values, the peak of the pole-dragging function y lies slightly below the peak of the cusp function (at $x = 1$) but still above the dividing line $1 - x$, so that Region 2 has a finite extent. Equally interesting is Region 3, between the lines $x = 1$ and where $y = 0$, in which the bare pole M_0 lies near threshold but is repelled by it nonetheless. Both of these effects are caused by the continuing attraction (to larger s values) of the cusp beyond $s_{\mathrm{th},i}$. From Fig. 2, one sees that the most effective dragging of the pole (the maximum of y) falls very close to the dividing line $y = 1 - x$, which is the point where $M_{\mathrm{pole}} = \sqrt{s_{\mathrm{th},i}}$.

We now turn to a direct comparison between the pole-dragging efficiency of diquark and mesonic cusps, which are chosen to have the same value of $s_{\mathrm{th},i}$. Of course, the presence of a cusplike structure not coinciding with a known mesonic threshold could suggest the presence of a distinct diquark threshold, possibly mixed with a δ-$\bar{\delta}$ resonance as discussed here, or even a heretofore unknown $\bar{q}q$ resonance; and even in the case that a meson and diquark threshold coincide or overlap, the shape of their combined effect would be distinct from that of a meson threshold alone. For the diquark form, the only free parameters are the coupling constant g_i and the bare pole mass as a multiple of threshold, $M_0/\sqrt{s_{\mathrm{th},i}}$. The mesonic cusp, on the other hand, contains the additional free parameter β_i indicative of a typical hadronic scale, which should assume roughly the same ≈0.5–1.0 GeV value for any hadronic system; alternately, it can be expressed [Eq. (18)] as the dimensionless combination μ_i, which changes from system to system depending on the value of $s_{\mathrm{th},i}$.

In Fig. 3 we compare the pole-dragging effectiveness parameter y of Eq. (28) as a function of $x \equiv M_0/\sqrt{s_{\mathrm{th},i}}$ for the choice $\sqrt{s_{\mathrm{th},i}} = m_{D^0} + m_{D^{*0}} = 3.872$ GeV relevant to the $X(3872)$. The diquark pole-dragging plot is identical to that in Fig. 2 (it is the dashed curve there), where it corresponds to $g_{i,\mathrm{diquark}} = 0.370$ GeV. The mesonic pole-dragging plots are presented for several values of β_i. Since, as discussed below, the values of $g_{i,\mathrm{diquark}}$ are chosen to scale with $g_{i,\mathrm{meson}}$ so that the diquark and mesonic cusp functions have the same height in each case, and since the absolute height of each mesonic pole-dragging curve changes with β_i, one should really view Fig. 3 as a family of plots: a diquark and a mesonic curve for each value of β_i. The diquark plots inherit β_i dependence only through this scaling. The diquark and mesonic plots give the indicated value of y only for $\beta_i = 1$ GeV (where $g_{i,\mathrm{meson}} = 0.474$ GeV), and both would be proportionally larger (smaller) for $\beta_i > 1$ GeV (< 1 GeV). However, for fixed $\sqrt{s_{\mathrm{th},i}}$ the diquark curves have a fixed shape and hence are scaled to the single (solid) curve in Fig. 3, while the mesonic curves become broader as β_i grows. They increase monotonically in width (and hence in pole-dragging effectiveness) as a function of β_i, achieving near parity with the diquark curve at $\beta_i = 1.7$ GeV. However, such a large value seems inconsistent with that expected from ordinary hadronic matter; if one limits to, e.g., values $\beta_i = 1.1$ GeV or less, then the mesonic curves are much

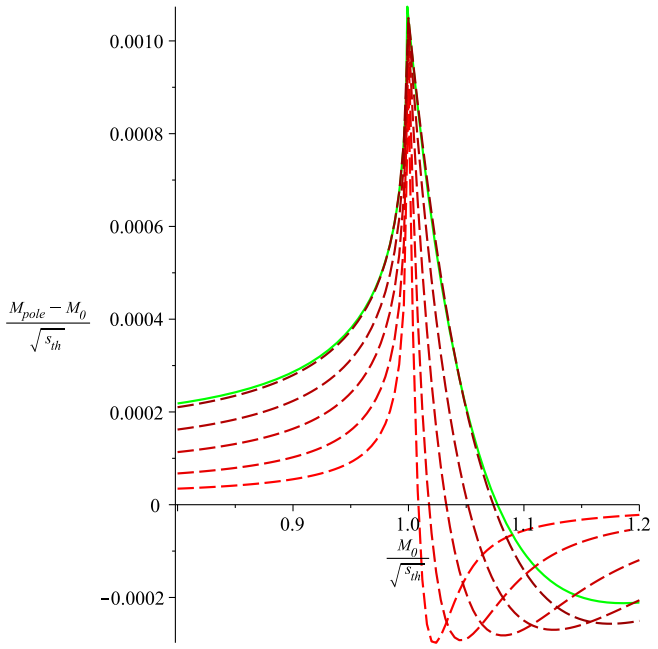

FIG. 3 (color online). Comparison of the effectiveness of pole dragging by cusps [y of Eq. (28)] as a function of $x \equiv M_0/\sqrt{s_{\mathrm{th},i}}$, as created by diquark (solid, green) and meson (dashed, red) thresholds. The values of β_i (in GeV) corresponding to the mesonic plots, in increasing width of the profile (or darkness of the shading), are 0.5, 0.8, 1.1, 1.4, and 1.7. The mesonic plots are scaled to the same cusp height, in the manner discussed in the text.

narrower than the diquark ones scaled to the same height, and hence mesonic thresholds do not drag resonant poles as effectively as diquark thresholds.

However, this very interesting result is also dependent upon the absolute size $s_{\mathrm{th},i}$ of the threshold. One expects the same range of β_i values to occur due to hadronic confinement physics, but the mesonic plots depend upon the dimensionless combination μ_i of Eq. (18). In the case of the $K\bar{K}$ threshold studied in Ref. [26], $\sqrt{s_{\mathrm{th},i}} = 0.991$ GeV, while for the studies of Z_b states in Ref. [29], the threshold is $\sqrt{s_{\mathrm{th},i}} = m_B + m_{B^*} = 10.604$ GeV.

One must also take into account the chosen size for the coupling constant g_i. In Fig. 3, the same cusp function peak value is used for both diquark and meson forms. Of course, no diquark pair production coupling constant has ever been measured experimentally; however, as noted in the Introduction, the fundamental strength of the color interaction between a qq pair forming a $\bar{\mathbf{3}}$ is fully half as strong as that between a $\bar{q}q$ pair forming a $\mathbf{1}$, so it is reasonable to take the diquark and meson g_i values to be comparable in size. In the plot captions, $g_{i,\mathrm{meson}}$ is the given numerical value, and $g_{i,\mathrm{diquark}}$ is derived from normalizing the peak of its cusp function to match that of the mesonic form; this ratio is computed using the values of $\pi_i(s_{\mathrm{th},i})$ in Eqs. (21) and (27).

Furthermore, the coupling g_i corresponds to the creation of hadrons containing heavy quarks of species Q (s for $K\bar{K}$, c for $D\bar{D}^*$, b for $B\bar{B}^*$) and therefore is proportional to the decay constant f_Q, which is known from heavy-quark effective theory to scale in terms of the heavy-quark mass m_Q as $1/\sqrt{m_Q}$. In turn, the relevant thresholds scale as $\sqrt{s_{\mathrm{th},i}} \sim m_Q$, so that $g_i \sim (s_{\mathrm{th},i})^{-1/4}$. The means by which all given coupling constants $g_{i,\mathrm{meson}}$ are given is therefore

$$g_i^2 = g_{K\bar{K}}^2 \sqrt{\frac{s_{\mathrm{th},K\bar{K}}}{s_{\mathrm{th},i}}}, \tag{29}$$

with $g_{K\bar{K}}^2 = 0.875$ GeV^2, an example given in Ref. [26]. Clearly, one may dispute treating the s quark as heavy, the accuracy of using $\sqrt{s_{\mathrm{th},i}}$ in place of m_Q, or indeed the scaling of diquark and meson cusp functions to have the same peak height. However, all of these issues may be adjusted to match one's prejudices by including appropriately chosen $O(1)$ correction coefficients. Our prescriptions are designed to make direct comparisons between the forms as clear as possible.

In Figs. 4, 5, and 6, we compare the pole-dragging effectiveness parameter y obtained for diquark thresholds, alongside the mesonic form with the $K\bar{K}$, $D\bar{D}^*$, and $B\bar{B}^*$ thresholds, respectively, each with $\beta_i = 1.0$ GeV. One sees that the $K\bar{K}$ mesonic curve is much wider than the diquark curve, while the $D\bar{D}^*$ and $B\bar{B}^*$ mesonic curves are much

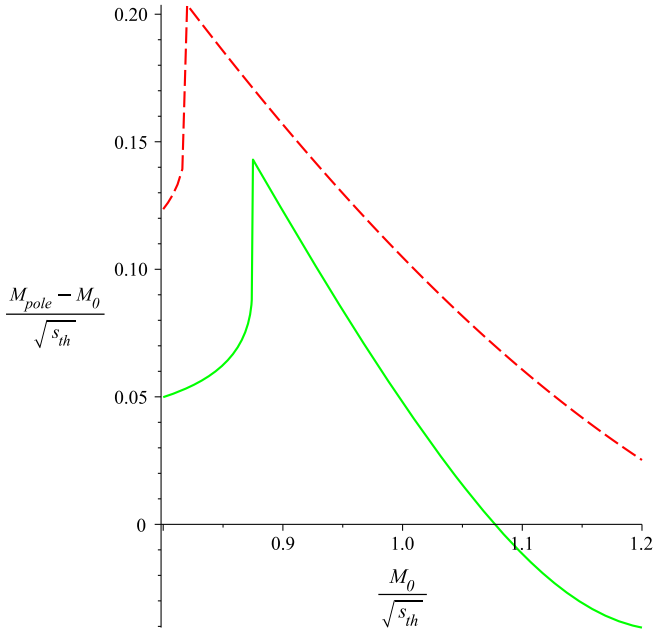

FIG. 4 (color online). Comparison of the effectiveness of pole dragging by cusps [y of Eq. (28)] as a function of $x \equiv M_0/\sqrt{s_{\mathrm{th},i}}$, from the diquark cusp (solid, green) and from the mesonic cusp (dashed, red) chosen to have $\beta_i = 1.0$ GeV. Here, $\sqrt{s_{\mathrm{th},i}} = 0.991$ GeV, and $g_{i,\mathrm{diquark}} = 1.348$ GeV, while $g_{i,\mathrm{meson}} = 0.935$ GeV to give the diquark and meson cusp functions the same height.

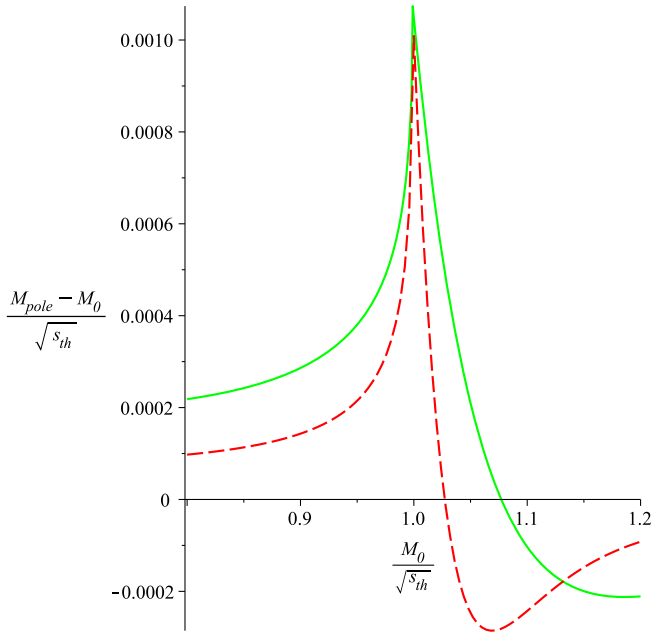

FIG. 5 (color online). As in Fig. 4, except with $\sqrt{s_{\mathrm{th},i}} = 3.872$ GeV, and $g_{i,\mathrm{diquark}} = 0.370$ GeV, while $g_{i,\mathrm{meson}} = 0.474$ GeV to give the diquark and meson cusp functions the same height. This case can be compared directly to that with $\beta = 1$ GeV in Fig. 3.

narrower. We infer that the presence of a δ-$\bar{\delta}$ threshold is more effective in dragging a resonant pole for heavy-quark systems, and the two-meson threshold is more effective in dragging a resonant pole for light-quark systems.

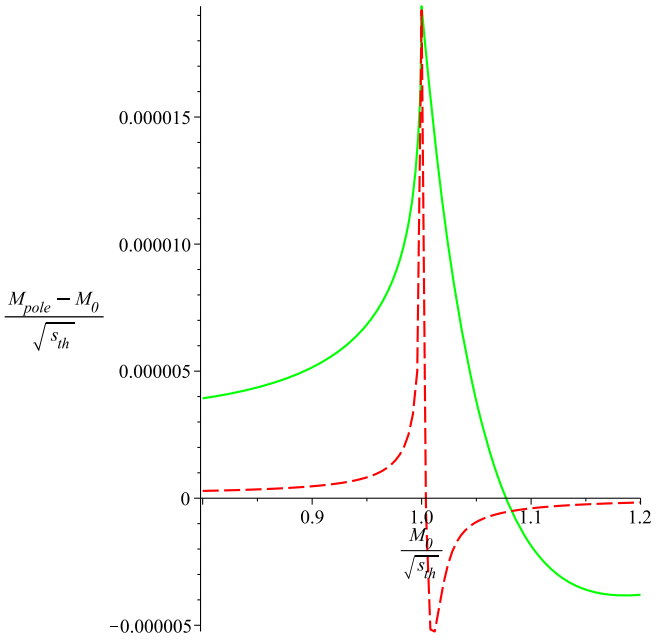

FIG. 6 (color online). As in Fig. 4, except with $\sqrt{s_{\mathrm{th},i}} = 10.604$ GeV, and $g_{i,\mathrm{diquark}} = 0.136$ GeV, while $g_{i,\mathrm{meson}} = 0.286$ GeV to give the diquark and meson cusp functions the same height.

But several other interesting results follow from Figs. 4, 5, and 6. First, the maximum height of the pole-dragging function y is much larger in the $K\bar{K}$ case than in the $D\bar{D}^*$ or $B\bar{B}^*$ cases, for either diquark or mesonic forms. Even taking into account the larger value of $\sqrt{s_{\mathrm{th},i}}$ for the latter cases, the absolute size of the maximal pole dragging is larger for the lighter cases; to wit, the numbers are about 200, 4.3, and 0.2 MeV, respectively. Some, but not all, of this decreased effectiveness can be attributed to the decrease of g_i via heavy-quark scaling given by Eq. (29). Indeed, for a fixed value of $s_{\mathrm{th},i}$, the relative size of the pole-dragging effect y is found empirically to scale approximately as g_i^2; clearly, the magnitude of $\sqrt{s_{\mathrm{th},i}}$ matters as well. In a related effect, the location of the peak in y travels a greater distance from threshold for lighter systems, and it is somewhat larger for the mesonic than the diquark effect, even when the cusp functions themselves have the same peak height. However, one should not conclude from these facts that the cusp effect is intrinsically less effective for heavy-quark systems; indeed, a number of the mass splittings between heavy hadrons scale as $1/m_Q$, so a full analysis would require one to take into account values of M_0 that lie naturally closer to $\sqrt{s_{\mathrm{th},i}}$.

VII. DISCUSSION AND CONCLUSIONS

We have performed the first analysis of the cusp effect due to the opening of diquark-antidiquark thresholds by using constituent counting rules to model their production form factor. We directly compared our results to those obtained from employing a frequently used phenomenologically based meson form factor and found that the magnitude of the pole-dragging effect is greater in both relative and absolute terms for lighter systems ($K\bar{K}$ vs $D\bar{D}^*$ or $B\bar{B}^*$). We also found that the effect due to mesonic cusps is larger than that due to diquark cusps for the $K\bar{K}$ threshold, while the diquark cusp effect is stronger for $D\bar{D}^*$ or $B\bar{B}^*$ thresholds.

This calculation is of course an idealization, in that only one threshold is present in each example; in reality, several thresholds, each with its own strength and contributing with different signs (due to the different Riemann sheets) are simultaneously present, and all contribute to the total effect. Furthermore, this calculation assumes, for maximum clarity of comparison, that the coupling constants for the diquark and mesonic cases give cusp functions of the same height and that the coupling constants scale with the thresholds according to expectations from heavy-quark effective theory. Any of these approximations can be relaxed in a more detailed analysis.

The central conclusion, however, is that, if δ-$\bar{\delta}$ states exist in the spectrum of QCD, then the opening of their production thresholds produces measurable shifts in the masses of resonances, which must be taken into account in precisely the same way as shifts appearing due to the opening of meson production thresholds. The cusp effect appears to promise a rich source of new physical effects.

ACKNOWLEDGMENTS

This work was supported by the National Science Foundation under Grants No. PHY-1068286 and No. PHY-1403891. R. F. L. thanks S. Brodsky and D. Bugg for encouragement and useful discussions and F.-K. Guo and C. Hanhart for interesting dialogue and insights.

APPENDIX: EXPRESSIONS FOR UNEQUAL MASSES

In the case $m_{1,i} \neq m_{2,i}$, let us define

$$m \equiv \frac{1}{2}(m_{1,i} + m_{2,i}),$$
$$\delta \equiv \frac{1}{2}(m_{1,i} - m_{2,i}),$$
$$\epsilon \equiv \frac{\delta^2}{m^2} \tag{A1}$$

and henceforth suppress the index i. Note that $s_{\mathrm{th},i} = 4m^2$. The kinematical variables are, in analog to Eqs. (3) and (7),

$$\rho = \frac{2k}{\sqrt{s}} = \sqrt{\left(1 - \frac{4m^2}{s}\right)\left(1 - \frac{4\delta^2}{s}\right)}, \tag{A2}$$

and its inverse reads

$$s = \frac{2m^2}{1-\rho^2}(1+\epsilon)(1+h), \tag{A3}$$

written in terms of the auxiliary variable

$$h \equiv \sqrt{1 - \frac{4\epsilon(1-\rho^2)}{(1+\epsilon)^2}}, \tag{A4}$$

which equals 1 in the equal-mass case $\epsilon = 0$. Analogous primed forms hold for $s \to s'$.

Then the generalization of Eq. (11) becomes

$$\pi(s) = \frac{1}{\pi}\mathrm{P}\int_0^1 d\rho' \frac{\rho'^2}{h'} \frac{F^2(s')}{(\frac{1-\rho^2}{1+h} - \frac{1-\rho'^2}{1+h'})}, \tag{A5}$$

and that of Eq. (13) is

$$\pi(s) = -\frac{1}{\pi}\int_0^1 d\rho' \left[F^2(s') + \frac{4m^2\rho'^2(1+\epsilon)(1+h')}{(1-\rho'^2)^2 h'}\frac{dF^2(s')}{ds'}\right] \times \ln\left|(1-\rho^2) - (1-\rho'^2)\frac{1+h}{1+h'}\right|. \tag{A6}$$

[1] R. Aaij *et al.* (LHCb Collaboration), Phys. Rev. Lett. **112**, 222002 (2014).
[2] S. K. Choi *et al.* (Belle Collaboration), Phys. Rev. Lett. **91**, 262001 (2003).
[3] N. Brambilla *et al.*, Eur. Phys. J. C **74**, 2981 (2014).
[4] A. Esposito, F. Piccinini, A. Pilloni, and A. D. Polosa, J. Mod. Phys. **04**, 1569 (2013).
[5] A. L. Guerrieri, F. Piccinini, A. Pilloni, and A. D. Polosa, Phys. Rev. D **90**, 034003 (2014).
[6] P. Artoisenet and E. Braaten, Phys. Rev. D **81**, 114018 (2010).
[7] P. Artoisenet and E. Braaten, Phys. Rev. D **83**, 014019 (2011).
[8] M. B. Voloshin, Prog. Part. Nucl. Phys. **61**, 455 (2008).
[9] L. Maiani, F. Piccinini, A. D. Polosa, and V. Riquer, Phys. Rev. D **71**, 014028 (2005).
[10] L. Maiani, F. Piccinini, A. D. Polosa, and V. Riquer, Phys. Rev. D **89**, 114010 (2014).
[11] S. J. Brodsky, D. S. Hwang, and R. F. Lebed, Phys. Rev. Lett. **113**, 112001 (2014).
[12] C.-Z. Yuan, Int. J. Mod. Phys. A **29**, 1430046 (2014).
[13] V. A. Matveev, R. M. Muradian, and A. N. Tavkhelidze, Lett. Nuovo Cimento **7**, 719 (1973).
[14] S. J. Brodsky and G. R. Farrar, Phys. Rev. Lett. **31**, 1153 (1973).
[15] S. J. Brodsky and G. R. Farrar, Phys. Rev. D **11**, 1309 (1975).
[16] G. R. Farrar and D. R. Jackson, Phys. Rev. Lett. **43**, 246 (1979).
[17] A. V. Efremov and A. V. Radyushkin, Teor. Mat. Fiz. **42**, 147 (1980) [Theor. Math. Phys. **42**, 97 (1980)].
[18] A. Duncan and A. H. Mueller, Phys. Rev. D **21**, 1636 (1980).
[19] A. Duncan and A. H. Mueller, Phys. Lett. B **93**, 119 (1980).
[20] G. P. Lepage and S. J. Brodsky, Phys. Rev. D **22**, 2157 (1980).
[21] D. W. Sivers, Annu. Rev. Nucl. Part. Sci. **32**, 149 (1982).
[22] A. H. Mueller, Phys. Rep. **73**, 237 (1981).
[23] S. J. Brodsky and G. P. Lepage, Adv. Ser. Direct. High Energy Phys. **5**, 93 (1989).
[24] S. J. Brodsky and R. F. Lebed, arXiv:1505.00803.
[25] N. A. Törnqvist, Z. Phys. C **68**, 647 (1995).
[26] D. V. Bugg, J. Phys. G **35**, 075005 (2008).
[27] F. K. Guo, C. Hanhart, Q. Wang, and Q. Zhao, Phys. Rev. D **91**, 051504 (2015).
[28] D. V. Bugg, Europhys. Lett. **96**, 11002 (2011).
[29] E. S. Swanson, Phys. Rev. D **91**, 034009 (2015).
[30] M. E. Peskin and D. V. Schroeder, *An Introduction to Quantum Field Theory* (Perseus, New York, 1995).

[31] H. Georgi, *Weak Interactions and Modern Particle Theory* (Dover, New York, 2009).
[32] C.-W. Hwang, Eur. Phys. J. C **23**, 585 (2002).
[33] J. Polchinski and M. J. Strassler, Phys. Rev. Lett. **88**, 031601 (2002).
[34] H. Kawamura, S. Kumano, and T. Sekihara, Phys. Rev. D **88**, 034010 (2013).
[35] H. Kawamura, S. Kumano, and T. Sekihara, JPS Conf. Proc. **1**, 013043 (2014).
[36] G. P. Lepage and S. J. Brodsky, Phys. Lett. B **87**, 359 (1979).
[37] A. V. Efremov and A. V. Radyushkin, Phys. Lett. B **94**, 245 (1980).
[38] V. V. Sudakov, Zh. Eksp. Teor. Fiz. **30**, 87 (1956) [Sov. Phys. JETP **3**, 65 (1956)].
[39] J. M. Cornwall and G. Tiktopoulos, Phys. Rev. D **13**, 3370 (1976).
[40] A. Sen, Phys. Rev. D **28**, 860 (1983).
[41] P. V. Landshoff, Phys. Rev. D **10**, 1024 (1974).
[42] H.-N. Li and G. F. Sterman, Nucl. Phys. **B381**, 129 (1992).
[43] A. P. Szczepaniak, arXiv:1501.01691.